# Decline of humoral responses against SARS-CoV-2 Spike in convalescent individuals

Guillaume Beaudoin-Bussières[1,2,*], Annemarie Laumaea[1,2,*], Sai Priya Anand[1,3,*], Jérémie Prévost[1,2,*], Romain Gasser[1,2,*], Guillaume Goyette[1], Halima Medjahed[1], Josée Perreault[4], Tony Tremblay[4], Antoine Lewin[4], Laurie Gokool[1], Chantal Morrisseau[1], Philippe Bégin[1,5], Cécile Tremblay[1,2], Valérie Martel-Laferrière[1,2], Daniel E. Kaufmann[1,6], Jonathan Richard[1,2], Renée Bazin[4] and Andrés Finzi[1,2,3,#]

[1]Centre de Recherche du CHUM, QC H2X 0A9, Canada
[2]Département de Microbiologie, Infectiologie et Immunologie, Université de Montréal, Montreal, QC H2X 0A9, Canada
[3]Department of Microbiology and Immunology, McGill University, Montreal, QC H3A 2B4, Canada
[4]Héma-Québec, Affaires Médicales et Innovation, Québec et Montréal, QC G1V 5C3, Canada
[5]CHU Ste-Justine, Montreal, QC, H3T 1C5, Canada
[6]Département de Médecine, Université de Montréal, Montreal, QC H2X 0A9, Canada

[*]Contributed equally

[#] Correspondence: andres.finzi@umontreal.ca

**Running Title: Antibodies against SARS-CoV-2 S in convalescent individuals**

**Key Words:** Coronavirus, COVID-19, SARS-CoV-2, Spike glycoproteins, D614G, RBD, ELISA, IgM, IgG, neutralization, cross-reactivity, convalescent plasma

**Word count for the abstract: 186**

**Word count for the text: 1105**

**ABSTRACT**

In the absence of effective vaccines and with limited therapeutic options, convalescent plasma is being collected across the globe for potential transfusion to COVID-19 patients. The therapy has been deemed safe and several clinical trials assessing its efficacy are ongoing. While it remains to be formally proven, the presence of neutralizing antibodies is thought to play a positive role in the efficacy of this treatment. Indeed, neutralizing titers of ≥1:160 have been recommended in some convalescent plasma trials for inclusion. Here we performed repeated analyses at one-month interval on 31 convalescent individuals to evaluate how the humoral responses against the SARS-CoV-2 Spike, including neutralization, evolve over time. We observed that receptor-binding domain (RBD)-specific IgG slightly decreased between six and ten weeks after symptoms onset but RBD-specific IgM decreased much more abruptly. Similarly, we observed a significant decrease in the capacity of convalescent plasma to neutralize pseudoparticles bearing SARS-CoV-2 S wild-type or its D614G variant. If neutralization activity proves to be an important factor in the clinical efficacy of convalescent plasma transfer, our results suggest that plasma from convalescent donors should be recovered rapidly after symptoms resolution.

## MAIN TEXT

Until an efficient vaccine to protect from SARS-CoV-2 infection is available, alternative approaches to treat or prevent acute COVID-19 are urgently needed. A promising approach is the use of convalescent plasma containing anti-SARS-CoV-2 antibodies collected from donors who have recovered from COVID-19 (1). Convalescent plasma therapy was successfully used in the treatment of SARS, MERS and influenza H1N1 pandemics and was associated with improvement of clinical outcomes (2-4). Experience to date shows that the passive transfer of convalescent plasma to acute COVID-19 patients has been shown to be well tolerated and presented some hopeful signs (5-9). In one study, the convalescent plasma used had high titers of IgG to SARS-CoV-2 (at least 1:1640), which correlated positively with neutralizing activity (10). While it remains to be formally demonstrated, neutralizing activity is considered an important determinant of convalescent plasma efficacy (11) and regulatory agencies have been recommending specific thresholds for qualifying convalescent plasma prior to its release. While neutralizing function has been associated with protection against reinfection in rhesus macaques (12), other antibody functions may be relevant for controlling an acute infection and should be examined to better understand the correlates of convalescent plasma-mediated efficacy (7).

It was recently reported that the humoral responses against SARS-CoV-2 are built rapidly, peaking at weeks 2 or 3 after symptoms onset but steadily decreases thereafter (13-15). Moreover, in a cross-sectional study we reported that the neutralization capacity decreased between the third and the sixth week after symptoms onset (14). Since convalescent patients are generally required to wait for 14 days after recovery to start plasma donations and that they may give multiple times in the following weeks, most donations are likely to occur even later than

this. Whether the neutralization capacity of convalescent plasma is stabilized after six weeks or decreases further remains unknown. To answer this question, which might have practical implications in the selection of plasma from convalescent donors, we analyzed serological samples from 31 convalescent donors collected at six and ten weeks after symptoms onset.

All convalescent donors initially tested positive for SARS-CoV-2 by RT-PCR on nasopharyngeal specimens with complete resolution of symptoms for at least 14 days before blood sampling. The average age of the donors was 46 years old (22 males and 9 females). We collected plasma samples from each individual at two time-points: 6 weeks after symptoms onset (baseline, median 43 days) and 4 weeks after (1 month, median 74 days after symptoms onset) (Supplemental Table 1).

We first evaluated the presence of RBD-specific IgG and IgM antibodies by ELISA as we recently described (14). In agreement with a recent report (16), we observed that both RBD-specific IgG and IgM titers significantly decreased between 6 and 10 weeks after symptoms onset. We noted that IgM titers diminished significantly more abruptly than IgG titers (Figure 1B and E respectively). Accordingly, the percentage of convalescent individuals presenting detectable titers of IgM decreased by ~13% at 10 weeks after symptoms onset (Figure 1C) while the percentage of infected individuals presenting detectable titers of IgG remained stable (Figure 1F).

We next used flow cytometry to examine the ability of convalescent plasma to recognize the full-length SARS-CoV-2 Spike expressed at the cell surface. Briefly, 293T cells expressing

SARS-CoV-2 S glycoproteins were stained with plasma samples, followed by incubation with secondary antibodies recognizing all antibody isotypes. Since the SARS-CoV-2 strain circulating in Europe and North America has the D614G mutation (17), we also evaluated recognition of this variant by flow cytometry. As presented in Supplemental Figure 1A, convalescent plasma from 96.8 % of donors (all but one) recognized both SARS-CoV-2 S (WT and D614G) at baseline. While this percentage remained stable four weeks later, the recognition (mean fluorescence intensity, MFI) was significantly diminished for both WT and D614G S-expressing cells, indicating that Spike-reactive antibodies were less abundant in convalescent plasma collected at this later time point. Interestingly, the MFI were almost identical for cells expressing the WT or D614G variant S (7206 and 7209 respectively, Fig. S1A), suggesting that the mutation did not significantly affect S conformation. In agreement with recent work, we observed that SARS-CoV-2-elicited antibodies cross-react with human *Sarbecoviruses* (14) (SARS-CoV; Figure S1B) and with another *Betacoronavirus* (OC43) whereas no cross-reactive antibodies to *Alphacoronavirus* (NL63, 229E) S glycoproteins (Figure S1C and S2) were detected. Cross-reactive antibodies recognizing SARS-CoV and OC43 S glycoproteins decreased between the two time-points following a trend similar to SARS-CoV-2 S-reactive antibodies.

We next measured the capacity of plasma samples to neutralize pseudoparticles bearing SARS-CoV-2 S, its D614G variant, SARS-CoV S or VSV-G glycoproteins using 293T cells stably expressing ACE2 as target cells (Figure 2). Neutralizing activity against SARS-CoV-2 WT or D614G S glycoprotein, as measured by the neutralization half-maximum inhibitory dilution ($ID_{50}$), was detected in 71% of patients six weeks after symptoms onset. SARS-CoV-2 neutralization was specific since no neutralization was observed against pseudoparticles

expressing VSV-G. Neutralizing activity against pseudoparticles bearing the SARS-CoV S glycoprotein was detected in only 25% of convalescent plasma and exhibited low potency, as previously reported (Figure 2) (14). Of note, while we observed enhanced infectivity for the D614G variant compared to its WT SARS-CoV-2 S counterpart (Figure S3A), no major differences in neutralization with convalescent plasma were detected at both time-points (Figure S3B), thus suggesting that the D614G change does not affect the overall conformation of the Spike, in agreement with recent findings (18).

The capacity to neutralize SARS-CoV-2 S WT or D614G-pseudotyped particles significantly correlated with the presence of RBD-specific IgG, IgM and anti-S antibodies (Figure S4). Interestingly, we observed a pronounced decrease (20-30%) in the percentage of patients able to neutralize pseudoparticles bearing SARS-CoV-2 S glycoprotein between 6 and 10 weeks after symptoms onset. Moreover, with plasma that still neutralized, the neutralization activity significantly decreased between these two time-points (Figure 2C). Interestingly, RBD-specific IgM and neutralizing activity declined more significantly in convalescent plasma overtime compared to RBD-specific IgG and anti-S Abs (Figure S5A, B). Moreover, while the loss of neutralizing activity on the WT and D614G pseudoparticles over time correlated with the loss of anti-RBD IgM and IgG antibodies, the correlation was higher for IgM than IgG (Figure S5C, D), suggesting that at least part of the neutralizing activity could be mediated by IgM, as recently proposed (13, 14).

In summary, our study indicates that plasma neutralization activity keeps decreasing passed the sixth week of symptom onset (14). It is currently unknown whether neutralizing

activity is truly driving the efficacy of convalescent plasma in acute COVID-19. If this was found to be the case, our results suggest that efforts should be made to ensure convalescent plasma is collected as soon as possible after recovery from active infection.

**ACKNOWLEDGMENTS**

The authors thank the convalescent plasma donors who participated in this study, the Héma-Québec team involved in convalescent donor recruitment and plasma collection, the CRCHUM BSL3 and Flow Cytometry Platforms for technical assistance, Dr Stefan Pöhlmann (Georg-August University, Germany) for the plasmids coding for SARS-CoV-2 S, 229E S and NL63 S glycoproteins, Dr Marcelline Côté (University of Ottawa) for the OC43 S expressor and Dr M. Gordon Joyce (U.S. MHRP) for the monoclonal antibody CR3022. This work was supported by le Ministère de l'Économie et de l'Innovation du Québec, Programme de soutien aux organismes de recherche et d'innovation to A.F and by the Fondation du CHUM. This work was also supported by a CIHR foundation grant #352417 to A.F. A.F. is the recipient of a Canada Research Chair on Retroviral Entry # RCHS0235 950-232424. G.B.B., S.P.A and J.P. are supported by CIHR fellowships. R.G. is supported by a MITACS Accélération postdoctoral fellowship. V.M.L. and P.B. are supported by FRQS Junior 1 salary awards. D.E.K. is a FRQS Merit Research Scholar. The funders had no role in study design, data collection and analysis, decision to publish, or preparation of the manuscript. The authors declare no competing interests.

## REFERENCES


1. **Chen L, Xiong J, Bao L, Shi Y.** 2020. Convalescent plasma as a potential therapy for COVID-19. Lancet Infect Dis **20:**398-400.

2. **Ko JH, Seok H, Cho SY, Ha YE, Baek JY, Kim SH, Kim YJ, Park JK, Chung CR, Kang ES, Cho D, Muller MA, Drosten C, Kang CI, Chung DR, Song JH, Peck KR.** 2018. Challenges of convalescent plasma infusion therapy in Middle East respiratory coronavirus infection: a single centre experience. Antivir Ther **23:**617-622.

3. **Hung IF, To KK, Lee CK, Lee KL, Chan K, Yan WW, Liu R, Watt CL, Chan WM, Lai KY, Koo CK, Buckley T, Chow FL, Wong KK, Chan HS, Ching CK, Tang BS, Lau CC, Li IW, Liu SH, Chan KH, Lin CK, Yuen KY.** 2011. Convalescent plasma treatment reduced mortality in patients with severe pandemic influenza A (H1N1) 2009 virus infection. Clin Infect Dis **52:**447-456.

4. **Cheng Y, Wong R, Soo YO, Wong WS, Lee CK, Ng MH, Chan P, Wong KC, Leung CB, Cheng G.** 2005. Use of convalescent plasma therapy in SARS patients in Hong Kong. Eur J Clin Microbiol Infect Dis **24:**44-46.

5. **Bloch EM, Shoham S, Casadevall A, Sachais BS, Shaz B, Winters JL, van Buskirk C, Grossman BJ, Joyner M, Henderson JP, Pekosz A, Lau B, Wesolowski A, Katz L, Shan H, Auwaerter PG, Thomas D, Sullivan DJ, Paneth N, Gehrie E, Spitalnik S, Hod EA, Pollack L, Nicholson WT, Pirofski LA, Bailey JA, Tobian AA.** 2020. Deployment of convalescent plasma for the prevention and treatment of COVID-19. J Clin Invest **130:**2757-2765.

6. **Casadevall A, Joyner MJ, Pirofski LA.** 2020. A Randomized Trial of Convalescent Plasma for COVID-19-Potentially Hopeful Signals. JAMA doi:10.1001/jama.2020.10218.

7. **Casadevall A, Pirofski LA.** 2020. The convalescent sera option for containing COVID-19. J Clin Invest **130:**1545-1548.

8. **Joyner MJ, Wright RS, Fairweather D, Senefeld JW, Bruno KA, Klassen SA, Carter RE, Klompas AM, Wiggins CC, Shepherd JR, Rea RF, Whelan ER, Clayburn AJ, Spiegel MR, Johnson PW, Lesser ER, Baker SE, Larson KF, Ripoll JG, Andersen KJ, Hodge DO, Kunze KL, Buras MR, Vogt MN, Herasevich V, Dennis JJ, Regimbal RJ, Bauer PR, Blair JE, van Buskirk CM, Winters JL, Stubbs JR, Paneth NS, Verdun NC, Marks P, Casadevall A.** 2020. Early safety indicators of COVID-19 convalescent plasma in 5,000 patients. J Clin Invest doi:10.1172/JCI140200.

9. **Duan K, Liu B, Li C, Zhang H, Yu T, Qu J, Zhou M, Chen L, Meng S, Hu Y, Peng C, Yuan M, Huang J, Wang Z, Yu J, Gao X, Wang D, Yu X, Li L, Zhang J, Wu X, Li B, Xu Y, Chen W, Peng Y, Hu Y, Lin L, Liu X, Huang S, Zhou Z, Zhang L, Wang Y, Zhang Z, Deng K, Xia Z, Gong Q, Zhang W, Zheng X, Liu Y, Yang H, Zhou D, Yu D, Hou J, Shi Z, Chen S, Chen Z, Zhang X, Yang X.** 2020. Effectiveness of convalescent plasma therapy in severe COVID-19 patients. Proc Natl Acad Sci U S A **117:**9490-9496.

10. **Li L, Zhang W, Hu Y, Tong X, Zheng S, Yang J, Kong Y, Ren L, Wei Q, Mei H, Hu C, Tao C, Yang R, Wang J, Yu Y, Guo Y, Wu X, Xu Z, Zeng L, Xiong N, Chen L, Wang J, Man N, Liu Y, Xu H, Deng E, Zhang X, Li C, Wang C, Su S, Zhang L, Wang J, Wu Y, Liu Z.** 2020. Effect of Convalescent Plasma Therapy on Time to

Clinical Improvement in Patients With Severe and Life-threatening COVID-19: A Randomized Clinical Trial. JAMA doi:10.1001/jama.2020.10044.

11. **Robbiani DF, Gaebler C, Muecksch F, Lorenzi JCC, Wang Z, Cho A, Agudelo M, Barnes CO, Gazumyan A, Finkin S, Hagglof T, Oliveira TY, Viant C, Hurley A, Hoffmann HH, Millard KG, Kost RG, Cipolla M, Gordon K, Bianchini F, Chen ST, Ramos V, Patel R, Dizon J, Shimeliovich I, Mendoza P, Hartweger H, Nogueira L, Pack M, Horowitz J, Schmidt F, Weisblum Y, Michailidis E, Ashbrook AW, Waltari E, Pak JE, Huey-Tubman KE, Koranda N, Hoffman PR, West AP, Jr., Rice CM, Hatziioannou T, Bjorkman PJ, Bieniasz PD, Caskey M, Nussenzweig MC.** 2020. Convergent antibody responses to SARS-CoV-2 in convalescent individuals. Nature doi:10.1038/s41586-020-2456-9.

12. **Deng W, Bao L, Liu J, Xiao C, Liu J, Xue J, Lv Q, Qi F, Gao H, Yu P, Xu Y, Qu Y, Li F, Xiang Z, Yu H, Gong S, Liu M, Wang G, Wang S, Song Z, Liu Y, Zhao W, Han Y, Zhao L, Liu X, Wei Q, Qin C.** 2020. Primary exposure to SARS-CoV-2 protects against reinfection in rhesus macaques. Science doi:10.1126/science.abc5343.

13. **Sterlin D, Mathian A, Miyara M, Mohr A, Anna F, Claer L, Quentric P, Fadlallah J, Ghillani P, Gunn C, Hockett R, Mudumba S, Guihot A, Luyt C-E, Mayaux J, Beurton A, Fourati S, Lacorte J-M, Yssel H, Parizot C, Dorgham K, Charneau P, Amoura Z, Gorochov G.** 2020. IgA dominates the early neutralizing antibody response to SARS-CoV-2. medRxiv doi:10.1101/2020.06.10.20126532**:**2020.2006.2010.20126532.

14. **Prévost J, Gasser R, Beaudoin-Bussières G, Richard J, Duerr R, Laumaea A, Anand SP, Goyette G, Ding S, Medjahed H, Lewin A, Perreault J, Tremblay T, Gendron-**

**Lepage G, Gauthier N, Carrier M, Marcoux D, Piché A, Lavoie M, Benoit A, Loungnarath V, Brochu G, Desforges M, Talbot PJ, Gould Maule GT, Côté M, Therrien C, Serhir B, Bazin R, Roger M, Finzi A.** 2020. Cross-sectional evaluation of humoral responses against SARS-CoV-2 Spike. bioRxiv doi:10.1101/2020.06.08.140244**:**2020.2006.2008.140244.

15. **Adams ER, Ainsworth M, Anand R, Andersson MI, Auckland K, Baillie JK, Barnes E, Beer S, Bell J, Berry T, Bibi S, Carroll M, Chinnakannan S, Clutterbuck E, Cornall RJ, Crook DW, De Silva T, Dejnirattisai W, Dingle KE, Dold C, Espinosa A, Eyre DW, Farmer H, Fernandez Mendoza M, Georgiou D, Hoosdally SJ, Hunter A, Jeffrey K, Klenerman P, Knight J, Knowles C, Kwok AJ, Leuschner U, Levin R, Liu C, Lopez-Camacho C, Martinez Garrido JC, Matthews PC, McGivern H, Mentzer AJ, Milton J, Mongkolsapaya J, Moore SC, Oliveira MS, Pereira F, Perez Lopez E, Peto T, Ploeg RJ, Pollard A, Prince T, et al.** 2020. Antibody testing for COVID-19: A report from the National COVID Scientific Advisory Panel. medRxiv doi:10.1101/2020.04.15.20066407**:**2020.2004.2015.20066407.

16. **Long QX, Tang XJ, Shi QL, Li Q, Deng HJ, Yuan J, Hu JL, Xu W, Zhang Y, Lv FJ, Su K, Zhang F, Gong J, Wu B, Liu XM, Li JJ, Qiu JF, Chen J, Huang AL.** 2020. Clinical and immunological assessment of asymptomatic SARS-CoV-2 infections. Nat Med doi:10.1038/s41591-020-0965-6.

17. **Korber B, Fischer W, Gnanakaran S, Yoon H, Theiler J, Abfalterer W, Foley B, Giorgi E, Bhattacharya T, Parker M, Partridge D, Evans C, de Silva T, LaBranche C, Montefiori D.** 2020. Spike mutation pipeline reveals the emergence of a more

transmissible form of SARS-CoV-2. bioRxiv doi:10.1101/2020.04.29.069054**:**2020.2004.2029.069054.

18. **Zhang L, Jackson CB, Mou H, Ojha A, Rangarajan ES, Izard T, Farzan M, Choe H.** 2020. The D614G mutation in the SARS-CoV-2 spike protein reduces S1 shedding and increases infectivity. bioRxiv doi:10.1101/2020.06.12.148726**:**2020.2006.2012.148726.

## Figure Legends

**Figure 1. SARS-CoV-2 RBD-specific IgM and IgG decrease over time.**

Indirect ELISA was performed using recombinant SARS-CoV-2 RBD and incubated with plasma samples recovered at baseline (6 weeks after symptoms onset; red lines) and 1 month later (black lines). Anti-RBD antibody binding was detected using (A-C) anti-IgM-HRP or (D-F) anti-IgG-HRP. Relative light units (RLU) obtained with BSA (negative control) were subtracted and further normalized to the signal obtained with the anti-RBD CR3022 mAb present in each plate. Data in graphs represent RLU (A,D) done in triplicate for each plasma or (B, E) the mean of the plasma recovered at baseline (red) and 1 month later (black). (C, F) Areas under the curve (AUC) were calculated based on RLU datasets shown in (A, D) using GraphPad Prism software and their average is shown on top of panels C and F, the percentage (%) of samples presenting a positive signal is indicated. Undetectable measures are represented as white symbols and limits of detection are plotted (calculated with samples from COVID-19 negative patients). Statistical significance was tested using Wilcoxon matched-pairs signed rank test (**** $p < 0.0001$).

**Figure 2. Neutralizing activity of convalescent plasma decreases over time.**

(A) Pseudoviral particles coding for the luciferase reporter gene and bearing the following glycoproteins: SARS-CoV-2 S or its D614G counterpart, SARS-CoV S and VSV-G were used to infect 293T-ACE2 cells. Pseudoviruses were incubated with serial dilutions of plasma samples recovered at baseline (6 weeks after symptoms onset) or collected 1 month later, at 37°C for 1h prior to infection of 293T-ACE2 cells. Infectivity at each dilution was assessed in duplicate and is shown as the percentage of infection without plasma for each pseudovirus. (B) The median of

neutralization by baseline (red) or 1 month (black) plasma samples is shown. (C) Neutralization half maximal inhibitory serum dilution ($ID_{50}$) values were determined using a normalized non-linear regression with Graphpad Prism software. Undetectable measures measures ($ID_{50}$< 50) are represented as white symbols. The mean neutralizing titers and the proportion (%) of neutralizer (patients with an ID50 over 50) are shown above the graphs. Statistical significance was tested using Wilcoxon matched-pairs signed rank tests (ns, not significant; **** $p < 0.0001$).

**SUPPLEMENTAL MATERIAL**

TEXT S1

FIG S1

FIG S2

FIG S3

FIG S4

FIG S5

TABLE S1

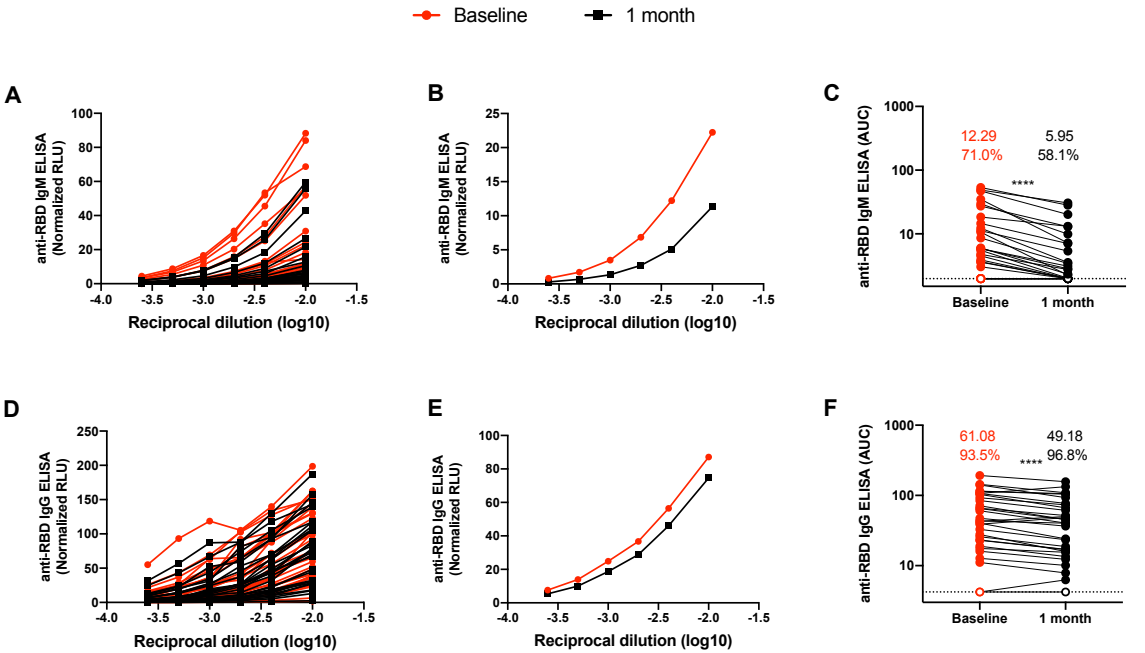


**Figure 1. SARS-CoV-2 RBD-specific IgM and IgG decrease over time.**
Indirect ELISA was performed using recombinant SARS-CoV-2 RBD and incubated with plasma samples recovered at baseline (6 weeks after symptoms onset; red lines) and 1 month later (black lines). Anti-RBD antibody binding was detected using (A-C) anti-IgM-HRP or (D-F) anti-IgG-HRP. Relative light units (RLU) obtained with BSA (negative control) were subtracted and further normalized to the signal obtained with the anti-RBD CR3022 mAb present in each plate. Data in graphs represent RLU (A,D) done in triplicate for each plasma or (B, E) the mean of the plasma recovered at baseline (red) and 1 month later (black). (C, F) Areas under the curve (AUC) were calculated based on RLU datasets shown in (A, D) using GraphPad Prism software and their average is shown on top of panels C and F, the percentage (%) of samples presenting a positive signal is indicated. Undetectable measures are represented as white symbols and limits of detection are plotted (calculated with samples from COVID-19 negative patients). Statistical significance was tested using Wilcoxon matched-pairs signed rank test (**** $p < 0.0001$).

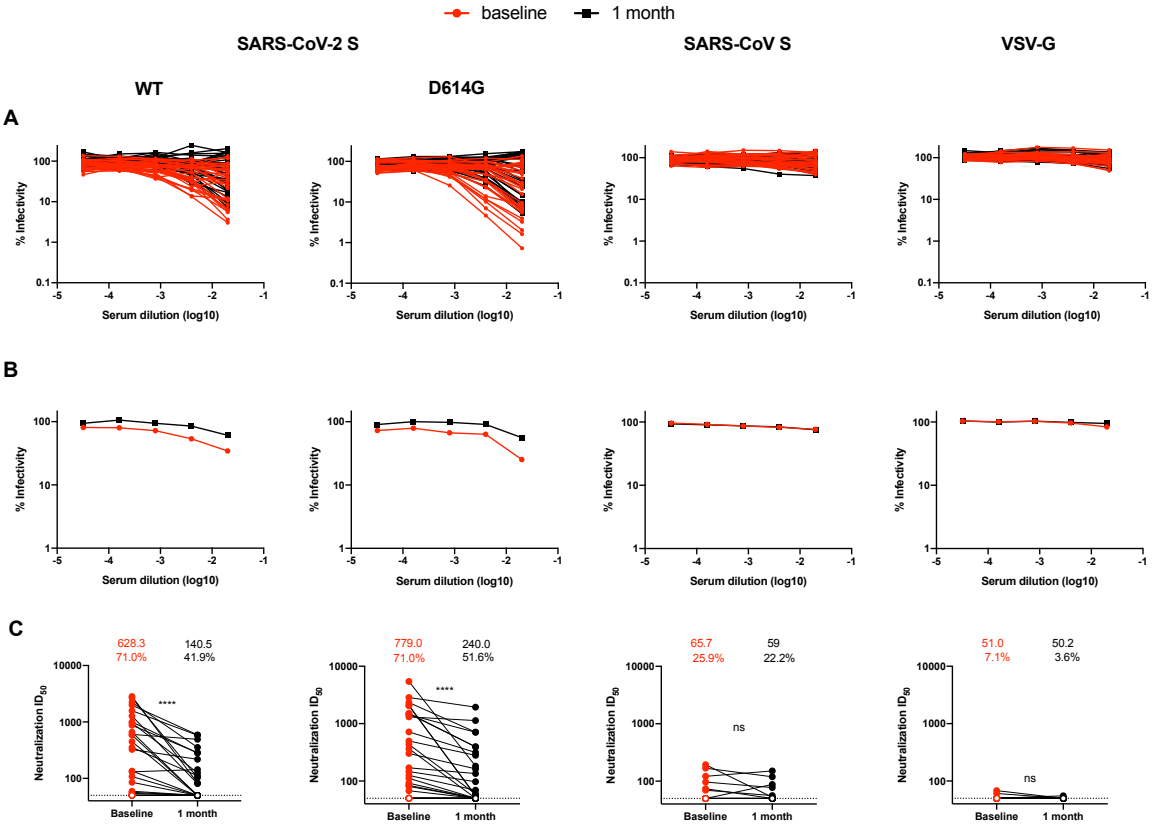


**Figure 2. Neutralizing activity of convalescent plasma decreases over time.**

(A) Pseudoviral particles coding for the luciferase reporter gene and bearing the following glycoproteins: SARS-CoV-2 S or its D614G counterpart, SARS-CoV S and VSV-G were used to infect 293T-ACE2 cells. Pseudoviruses were incubated with serial dilutions of plasma samples recovered at baseline (6 weeks after symptoms onset) or collected 1 month later, at 37°C for 1h prior to infection of 293T-ACE2 cells. Infectivity at each dilution was assessed in duplicate and is shown as the percentage of infection without plasma for each pseudovirus. (B) The median of neutralization by baseline (red) or 1 month (black) plasma samples is shown. (C) Neutralization half maximal inhibitory serum dilution ($ID_{50}$) values were determined using a normalized non-linear regression with Graphpad Prism software. Undetectable measures measures ($ID_{50}$ under 50) are represented as white symbols. The mean neutralizing titers and the proportion (%) of neutralizer (patients with an $ID_{50}$ over 50) are shown above the graphs. Statistical significance was tested using Wilcoxon matched-pairs signed rank tests (ns, not significant; **** $p < 0.0001$).

## SUPPLEMENTAL MATERIAL AND METHODS

### Ethics statement

All work was conducted in accordance with the Declaration of Helsinki in terms of informed consent and approval by an appropriate institutional board. Convalescent plasmas were obtained from donors who consented to participate in this research project at Héma-Québec (REB # 2020-004) and CHUM (19.381). The donors met all donor eligibility criteria: previous confirmed COVID-19 infection and complete resolution of symptoms for at least 14 days.

### Plasmids

The plasmids expressing the human coronavirus Spikes of SARS-CoV-2, SARS-CoV, NL63 229E (1, 2) and OC43 (3) were previously described. The D614G mutation was introduced using the QuikChange II XL site-directed mutagenesis protocol (Stratagene). The presence of the desired mutations was determined by automated DNA sequencing. The plasmid encoding for SARS-CoV-2 S RBD was synthesized commercially by Genscript. The RBD sequence (encoding for residues 319-541) fused to a C-terminal hexahistidine tag was cloned into the pcDNA3.1(+) expression vector. The vesicular stomatitis virus G (VSV-G)-encoding plasmid (pSVCMV-IN-VSV-G) was previously described (4).

### Cell lines

293T human embryonic kidney cells (obtained from ATCC) were maintained at 37°C under 5% $CO_2$ in Dulbecco's modified Eagle's medium (DMEM) (Wisent) containing 5% fetal bovine serum

(VWR), 100 UI/ml of penicillin and 100µg/ml of streptomycin (Wisent). 293T-ACE2 cell line was previously reported (3).

**Protein expression and purification**

FreeStyle 293F cells (Invitrogen) were grown in FreeStyle 293F medium (Invitrogen) to a density of 1 x $10^6$ cells/mL at 37°C with 8 % CO2 with regular agitation (150 rpm). Cells were transfected with a plasmid coding for SARS-CoV-2 S RBD using ExpiFectamine 293 transfection reagent, as directed by the manufacturer (Invitrogen). One week later, cells were pelleted and discarded. Supernatants were filtered using a 0.22 µm filter (Thermo Fisher Scientific). The recombinant RBD proteins were purified by nickel affinity columns, as directed by the manufacturer (Invitrogen). The RBD preparations were dialyzed against phosphate-buffered saline (PBS) and stored in aliquots at -80°C until further use. To assess purity, recombinant proteins were loaded on SDS-PAGE gels and stained with Coomassie Blue.

**Plasma and antibodies**

Plasma from SARS-CoV-2-infected and uninfected donors were collected, heat-inactivated for 1 hour at 56 °C and stored at -80°C until ready to use in subsequent experiments. Plasma from uninfected donors were used as negative controls and used to calculate the seropositivity threshold in our ELISA and flow cytometry assays. The monoclonal antibody CR3022 was used as a positive control in ELISA assays and was previously described (5-7). Horseradish peroxidase (HRP)-conjugated antibody specific for the Fc region of human IgG (Invitrogen) or for the Fc region of human IgM (Jackson ImmunoResearch Laboratories, inc.) were used as secondary antibodies to detect antibody binding in ELISA experiments. Alexa Fluor-647-conjugated goat

anti-human IgG (H+L) Abs (Invitrogen) were used as secondary antibodies to detect sera binding in flow cytometry experiments.

**ELISA**

The SARS-CoV-2 RBD assay used was recently described (3). Briefly, recombinant SARS-CoV-2 S RBD proteins (2.5 μg/ml), or bovine serum albumin (BSA) (2.5 μg/ml) as a negative control, were prepared in PBS and were adsorbed to plates (MaxiSorp; Nunc) overnight at 4°C. Coated wells were subsequently blocked with blocking buffer (Tris-buffered saline [TBS] containing 0.1% Tween20 and 2% BSA) for 1h at room temperature. Wells were then washed four times with washing buffer (Tris-buffered saline [TBS] containing 0.1% Tween20). CR3022 mAb (50ng/ml) or serial dilutions of plasma from SARS-CoV-2-infected or uninfected donors (1/100; 1/250; 1/500; 1/1000; 1/2000; 1/4000) were prepared in a diluted solution of blocking buffer (0.1 % BSA) and incubated with the RBD-coated wells for 90 minutes at room temperature. Plates were washed four times with washing buffer followed by incubation with secondary Abs (diluted in a diluted solution of blocking buffer (0.4% BSA)) for 1h at room temperature, followed by four washes. HRP enzyme activity was determined after the addition of a 1:1 mix of Western Lightning oxidizing and luminol reagents (Perkin Elmer Life Sciences). Light emission was measured with a LB941 TriStar luminometer (Berthold Technologies). Signal obtained with BSA was subtracted for each plasma and was then normalized to the signal obtained with CR3022 mAb present in each plate. The seropositivity threshold was established using the following formula: mean of all COVID-19 negative plasmas + (3 standard deviation of the mean of all COVID-19 negative plasmas).

**Flow cytometry analysis of cell-surface staining**

Using the standard calcium phosphate method, 10µg of Spike expressor and 2µg of a green fluorescent protein (GFP) expressor (pIRES-GFP) were transfected into $2 \times 10^6$ 293T cells. At 48h post transfection, 293T cells were stained with plasma from SARS-CoV-2-infected or uninfected individuals (1:250 dilution). The percentage of transfected cells (GFP+ cells) was determined by gating the living cell population based on the basis of viability dye staining (Aqua Vivid, Invitrogen). Samples were acquired on a LSRII cytometer (BD Biosciences, Mississauga, ON, Canada) and data analysis was performed using FlowJo vX.0.7 (Tree Star, Ashland, OR, USA). The seropositivity threshold was established using the following formula: mean of all COVID-19 negative plasmas + (3 standard deviation of the mean of all COVID-19 negative plasma + inter-assay coefficient of variability).

**Virus neutralization assay**

293T-ACE2 target cells were infected with single-round luciferase-expressing lentiviral particles. Briefly, 293T cells were transfected by the calcium phosphate method with the lentiviral vector pNL4.3 R-E- Luc (NIH AIDS Reagent Program) and a plasmid encoding for SARS-CoV-2 Spike (WT or D614G), SARS-CoV Spike or VSV-G at a ratio of 5:4. Two days post-transfection, cell supernatants were harvested and stored at –80°C until use. 293T-ACE2 target cells were seeded at a density of $1\times10^4$ cells/well in 96-well luminometer-compatible tissue culture plates (Perkin Elmer) 24h before infection. Recombinant viruses in a final volume of 100µl were incubated with the indicated plasma dilutions (1/50; 1/250; 1/1250; 1/6250; 1/31250) for 1h at 37°C and were then added to the target cells followed by incubation for 48h at 37°C; cells were lysed by the addition of 30µl of passive lysis buffer (Promega) followed by one freeze-thaw cycle. An LB941

TriStar luminometer (Berthold Technologies) was used to measure the luciferase activity of each well after the addition of 100µl of luciferin buffer (15mM $MgSO_4$, 15mM $KPO_4$ [pH 7.8], 1mM ATP, and 1mM dithiothreitol) and 50µl of 1mM d-luciferin potassium salt (Prolume). The neutralization half-maximal inhibitory dilution ($ID_{50}$) represents the plasma dilution to inhibit 50% of the infection of 293T-ACE2 cells by recombinant viruses bearing the indicated surface glycoproteins.

**Statistical analyses**

Statistics were analyzed using GraphPad Prism version 8.0.2 (GraphPad, San Diego, CA, (USA). Every data set was tested for statistical normality and this information was used to apply the appropriate (parametric or nonparametric) statistical test. P values <0.05 were considered significant; significance values are indicated as * P<0.05, ** P<0.01, *** P<0.001, **** P<0.0001.

## References


1. **Hoffmann M, Kleine-Weber H, Schroeder S, Kruger N, Herrler T, Erichsen S, Schiergens TS, Herrler G, Wu NH, Nitsche A, Muller MA, Drosten C, Pohlmann S.** 2020. SARS-CoV-2 Cell Entry Depends on ACE2 and TMPRSS2 and Is Blocked by a Clinically Proven Protease Inhibitor. Cell **181:**271-280 e278.
2. **Hofmann H, Pyrc K, van der Hoek L, Geier M, Berkhout B, Pohlmann S.** 2005. Human coronavirus NL63 employs the severe acute respiratory syndrome coronavirus receptor for cellular entry. Proc Natl Acad Sci U S A **102:**7988-7993.
3. **Prévost J, Gasser R, Beaudoin-Bussières G, Richard J, Duerr R, Laumaea A, Anand SP, Goyette G, Ding S, Medjahed H, Lewin A, Perreault J, Tremblay T, Gendron-Lepage G, Gauthier N, Carrier M, Marcoux D, Piché A, Lavoie M, Benoit A, Loungnarath V, Brochu G, Desforges M, Talbot PJ, Gould Maule GT, Côté M, Therrien C, Serhir B, Bazin R, Roger M, Finzi A.** 2020. Cross-sectional evaluation of humoral responses against SARS-CoV-2 Spike. bioRxiv doi:10.1101/2020.06.08.140244**:**2020.2006.2008.140244.
4. **Lodge R, Lalonde JP, Lemay G, Cohen EA.** 1997. The membrane-proximal intracytoplasmic tyrosine residue of HIV-1 envelope glycoprotein is critical for basolateral targeting of viral budding in MDCK cells. EMBO J **16:**695-705.
5. **ter Meulen J, van den Brink EN, Poon LL, Marissen WE, Leung CS, Cox F, Cheung CY, Bakker AQ, Bogaards JA, van Deventer E, Preiser W, Doerr HW, Chow VT, de Kruif J, Peiris JS, Goudsmit J.** 2006. Human monoclonal antibody combination against SARS coronavirus: synergy and coverage of escape mutants. PLoS Med **3:**e237.

6. **Yuan M, Wu NC, Zhu X, Lee CD, So RTY, Lv H, Mok CKP, Wilson IA.** 2020. A highly conserved cryptic epitope in the receptor binding domains of SARS-CoV-2 and SARS-CoV. Science **368:**630-633.

7. **Tian X, Li C, Huang A, Xia S, Lu S, Shi Z, Lu L, Jiang S, Yang Z, Wu Y, Ying T.** 2020. Potent binding of 2019 novel coronavirus spike protein by a SARS coronavirus-specific human monoclonal antibody. Emerg Microbes Infect **9:**382-385.

**Supplemental Table 1. Cohort characteristics.**

| Time after symptoms onset and first sample collection : Baseline (Median; Days; Day range) | Time after symptoms onset and second sample collection : 1 month (Median; Days; Day range) | Age (Average; Years; Age range) | Sex | |
|---|---|---|---|---|
| | | | Male (n) | Female (n) |
| 43 (16-60) | 74 (44-87) | 46 (20-67) | 22 | 9 |

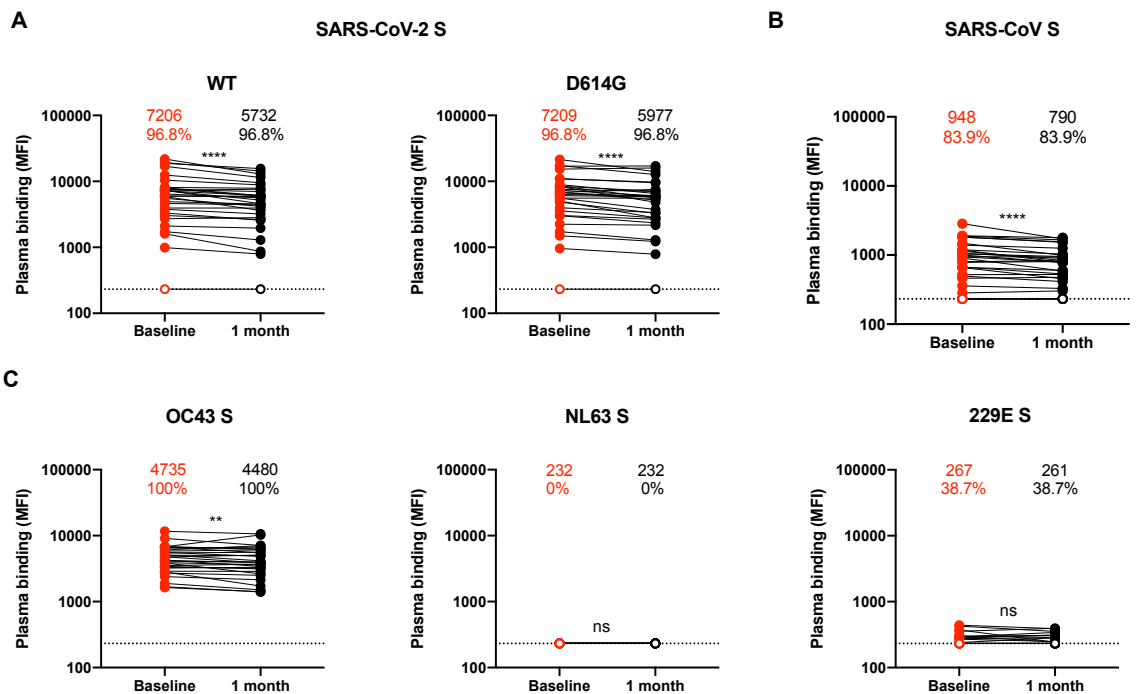


**Figure S1. Cross-reactive antibodies against human *Betacoronaviruses* decrease over time.**
Cell-surface staining of 293T cells expressing full-length Spike (S) from different HCoV (A) SARS-CoV-2 or its D614G counterpart (B), SARS-CoV, (C) OC43, NL63 and 229E with plasma samples recovered at baseline (6 weeks after symptoms onset) and 1 month later. The graphs shown represent the median fluorescence intensities (MFI). Undetectable measures are represented as white symbols and limits of detection are plotted. The average MFI and percentage (%) of positive samples is indicated in top of each panel. Statistical significance was tested using Wilcoxon matched-pairs signed rank test (ns, not significant; ** $p < 0.01$; **** $p < 0.0001$).

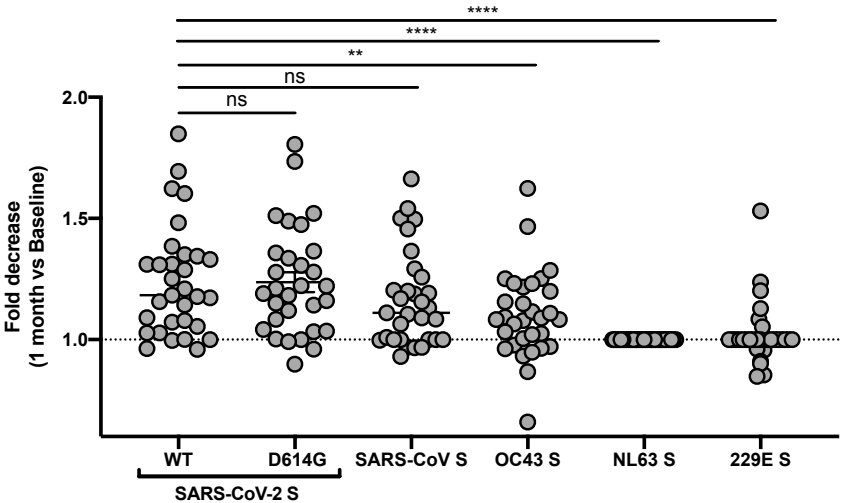


**Figure S2. Decrease in cross-reactive antibodies**

Fold decrease (1 month vs baseline) of the capacity of plasma to recognize by flow cytometry SARS-CoV-2 S WT, SARS-CoV-2 S D614G, SARS-CoV S, OC43 S, NL63 S and 229E S glycoproteins expressed at the surface of 293T cells. Statistical significance was tested using Wilcoxon matched-pairs signed rank tests (ns, not significant; ** $p < 0.01$; **** $p < 0.0001$).

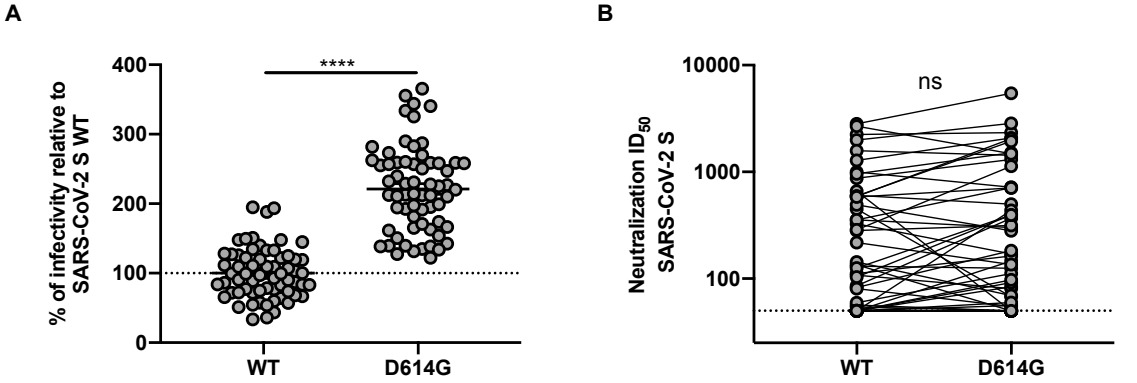


**Figure S3. D614G mutation enhances SARS-CoV-2 infectivity but does not affect its susceptibility to plasma neutralization.**(A) Reverse Transcriptase normalized levels of pseudoviral particles bearing the SARS-CoV-2 S WT or D614G variant were used to infect 293T/ACE2 cells and infectivity measured 48h later by luciferase activity. Graph shown represents the percentage of infectivity relative to pseudoviral particle bearing the SARS-CoV-2 S WT. Statistical significance was tested using Mann-Whitney U tests (**** $p < 0.0001$). (B) Comparison between the neutralization $ID_{50}$ from pseudoparticles bearing SARS-CoV-2 S WT and SARS-CoV-2 S D614G. Statistical significance was tested using Wilcoxon matched-pairs signed rank test. (ns, not significant).

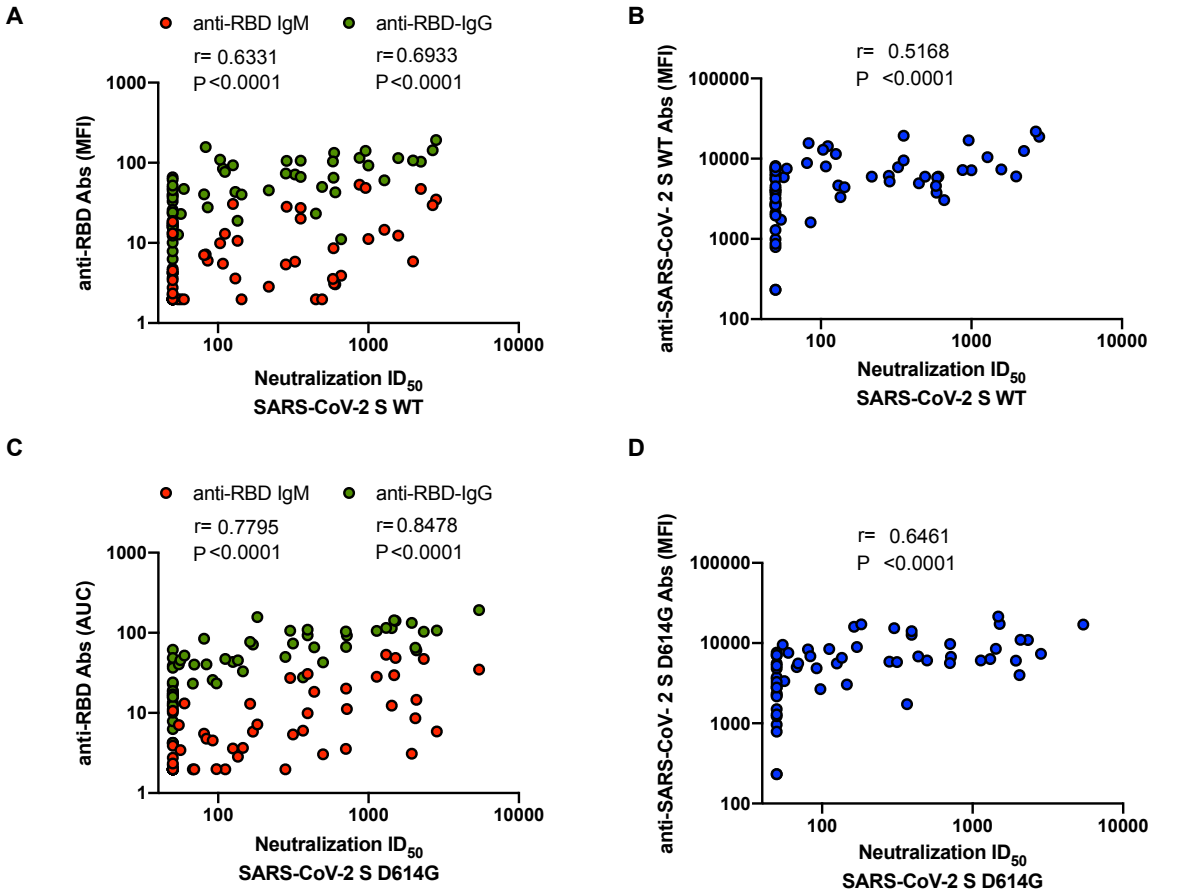


**Figure S4. SARS-CoV-2 RBD and full length S specific antibodies correlate with pseudoviruses neutralization.** Anti-RBD IgG and IgM evaluated by ELISA (A, C) or anti-S antibodies evaluated by flow cytometry (B, D) were plotted against the levels of neutralization ($ID_{50}$) of pseudoparticles bearing the SARS-CoV-2 S (A, B) or its D614G counterpart (C, D). Statistical analysis was performed using Spearman rank correlation tests.

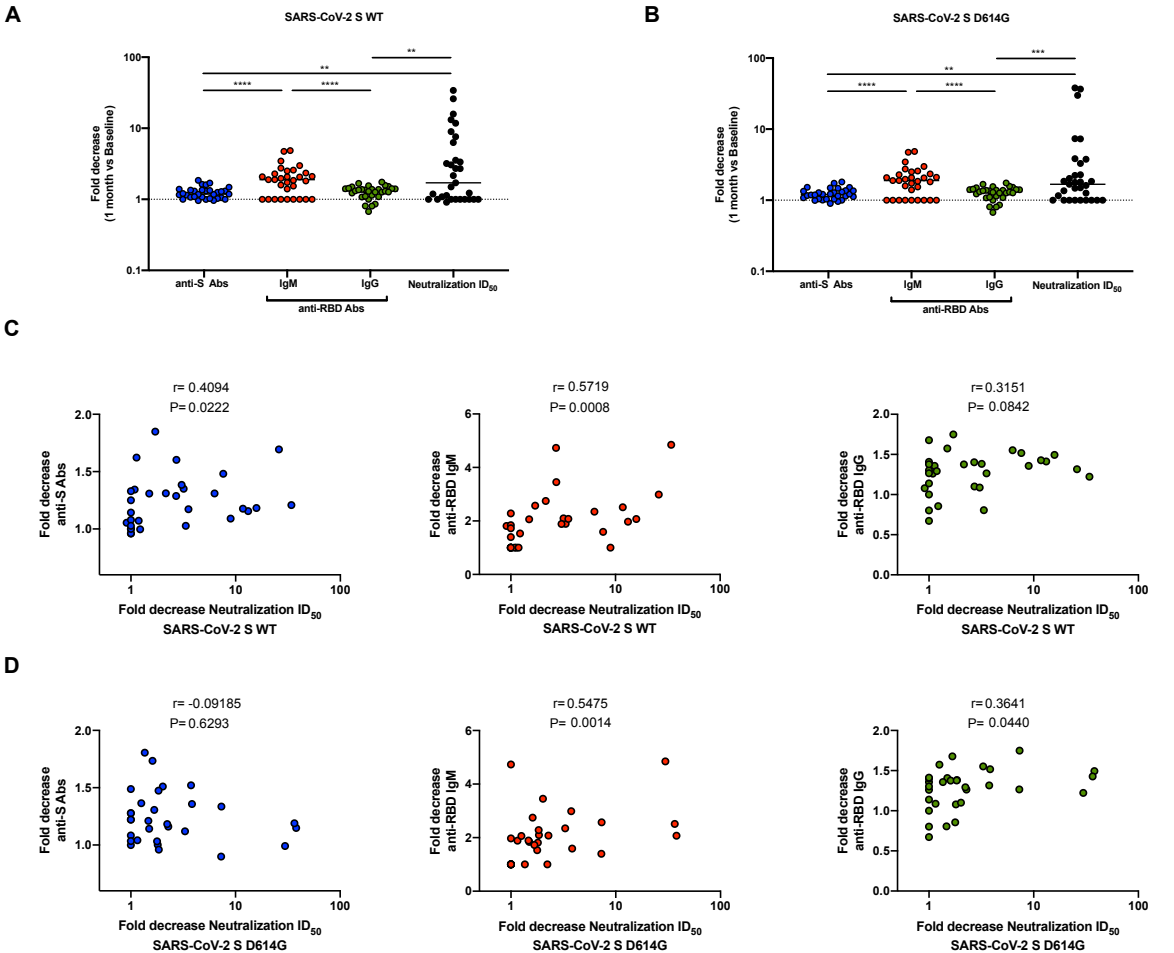


**Figure S5. Decrease in anti-RBD IgM antibodies over time correlates with reduced neutralizing activity.**
Fold decrease of the 31 pairs of plasma over the course of 1 month (1 month over Baseline) of the levels of anti-SARS-CoV-2 S WT or D614G antibodies quantified by flow cytometry, anti-RBD antibodies (IgM and IgG) quantified by ELISA and of neutralization $ID_{50}$ with pseudoparticules bearing (A) SARS-CoV-2 S WT or (B) SARS-CoV-2 S D614G. Correlation between the fold decrease over the course of 1 month of anti-SARS-CoV-2 S WT or D614G antibodies quantified by flow cytometry, anti-RBD (IgM and IgG) antibodies quantified by ELISA and the fold decrease of the neutralization $ID_{50}$ of pseudoparticules bearing (C) SARS-CoV-2 S WT or (D) SARS-CoV-2 S D614G. (A, B) Statistical significance was tested using Wilcoxon matched-pairs signed rank tests (** $p < 0.01$; *** $p < 0.001$; **** $p < 0.0001$). (C, D) Statistical significance was tested using Spearman rank correlation tests.